Upconversion of partition noise in semiconductors operating under periodic large-signal conditions

P. Shiktorov, E. Starikov, and V. Gružinskis
Semiconductor Physics Institute, A. Goštauto 11, 2600 Vilnius, Lithuania

S. Pérez and T. González
Departamento de Física Aplicada, Universidad de Salamanca, Plaza de la Merced s/n, 37008 Salamanca, Spain

L. Reggiani
INFM - National Nanotechnology Laboratory, Dipartimento di Ingegneria dell' Innovazione, Università di Lecce, Via Arnesano s/n, 73100 Lecce, Italy

L. Varani and J. C. Vaissière
Centre d'Electronique et de Micro-optoélectronique de Montpellier (CNRS UMR 5507), Université Montpellier II, 34095 Montpellier Cedex 5, France

(Received 17 June 2002; revised manuscript received 17 October 2002; published 10 April 2003)

By means of Monte Carlo simulations of bulk semiconductors operating in the periodic large-signal regime, we show the existence of upconversion of hot-carrier partition noise associated with the fluctuations between different groups of carriers in momentum space, characterized by different dynamical properties. The signature of the upconversion phenomenon is predicted by an analytical model and confirmed by the spectral analysis of the instantaneous spectral density of velocity fluctuations. As applications, we investigate the cases in which the two groups of carriers pertain to a single band in the presence of strong low-temperature optical-phonon emission and to lowest- and upper-valley populations in compound semiconductors.

DOI: 10.1103/PhysRevB.67.165201 PACS number(s): 72.70.+m, 72.20.Ht, 72.30.+q

I. INTRODUCTION

The notion of *partition noise* was first introduced for multigrid vacuum tubes, where this class of noise is generated due to random distribution of electrons and, hence, electrical currents between various positive electrodes.[1] Thus, in this case the noise is caused by carrier number fluctuations between different groups of carriers located in real space. By contrast, in semiconductor materials and devices the partition noise results from random transitions of carriers between two or more physically distinct groups of electron states located in momentum space.[2–5] For such a subdivision into groups to take place, the characteristic time of carrier exchange between groups must be much longer than that for intragroup transitions. The usual physical examples are the trapping-detrapping processes and intervalley transitions in multivalley semiconductors (intervalley noise). For two groups of carriers, the partition noise is characterized by a simple Lorentzian spectrum:[2–5] $S(\omega)=S(0)/[1+\omega^2\tau_g^2]$, where τ_g is the characteristic time of the intergroup transfer. In usual conditions, partition noise can manifest itself merely as a low-frequency noise at $\omega \leqslant \tau_g^{-1}$. In the low-frequency region, the presence of other noise contributions originated by other mechanisms complicates significantly the investigation of partition noise not only experimentally but also theoretically, when direct statistical simulations of noise phenomena, for example, by Monte Carlo (MC) methods, are used.

It is well known that in the presence of a periodic signal of given amplitude an excess low-frequency noise component can be transferred to a high-frequency region of the spectrum centered around the frequency of the periodic signal and its harmonics (the so-called *upconversion* of noise). Typical examples are the transfer of $1/f$ or generation-recombination low-frequency noise to the GHz region in voltage-controlled oscillators[6] and systems driven by periodic large-amplitude excitations.[7–9] One can expect similar upconversion phenomena appearing under hot-carrier conditions when the carrier distribution in momentum space can be decomposed into two or more parts (groups), each of them with a quasi-independent dynamics of motion. The aim of this paper is to theoretically investigate such a possibility by means of MC simulations of hot-carrier noise when a harmonic microwave electric field (MWEF) is applied to bulk semiconductors. For this sake, we first consider a simplified model of partition-noise upconversion to obtain the signature of the upconversion phenomenon within an analytical approach (Sec. II). Then, by MC simulations we investigate two cases of relevant physical interest when at least two groups of carriers can appear under hot-carrier conditions (Sec. III). The procedure for the noise analysis is based on MC calculations of the two-time symmetric correlation function as detailed in Ref. 10. The signature of noise upconversion will be analyzed and validated by comparing the results of the simulations with those of the analytical model. The main conclusions will be presented in Sec. IV.

II. MODEL

Here we use the conventional definition of diffusion noise source as applied to semiconductor materials and devices. It implies that an initial (primitive) fluctuation takes place only in momentum space and originates from the instantaneous scattering of a carrier with lattice imperfections (impurities, phonons, etc.).[11] As a consequence, fluctuations in real space

must be considered as induced by a primitive random process in momentum space. To single out such a peculiarity of the diffusion noise source, the instantaneous carrier distribution function, $f(\mathbf{p},x,t)$, is usually factorized with respect to real and momentum spaces as

$$f(\mathbf{p},x,t)=F(\mathbf{p},x,t)n(x,t), \tag{1}$$

where $n(x,t)$ and $F(\mathbf{p},x,t)$ are, respectively, the carrier concentration and the density of the momentum distribution of carriers placed at time t in the neighborhood of point x in real space (for simplicity, one-dimensional real space is considered). The representation of $f(\mathbf{p},x,t)$ given by Eq. (1) assumes the invariance in time and space of the normalization of $F(\mathbf{p},x,t)$ given by

$$\int_{\Omega} F(\mathbf{p},x,t)d\mathbf{p}=1, \tag{2}$$

where Ω is the whole momentum space. Since during a scattering event only the carrier momentum is changed, carrier scatterings are equivalent to spontaneous fluctuations of $F(\mathbf{p},x,t)$ which do not violate its normalization given by Eq. (2). At a macroscopic level it is convenient to describe such fluctuations as fluctuations of the drift velocity,

$$v_d(x,t)=\int_{\Omega} v(\mathbf{p})F(\mathbf{p},x,t)d\mathbf{p}, \tag{3}$$

where $v(\mathbf{p})$ is the carrier group velocity depending on the value of the momentum $\mathbf{p}$. To exclude from further consideration fluctuations of $v_d(x,t)$ induced by the self-consistent electric field and nonlocal effects appearing on the mean-free-path length scale, let us consider the case of an homogeneous semiconductor with frozen, i.e., constant in time and space, carrier concentration $n(x,t)=\text{const}$. In such a case, the fluctuations of the drift velocity $v_d(t)$ with respect to the statistical average value $\overline{v_d}$, $\delta v_d(t)=v_d(t)-\overline{v_d}$, are caused only by scattering events, which is the condition under which they can be considered as the primitive source of diffusion noise.

Let us subdivide the momentum space into two nonoverlapping volumes (groups) Ω_1 and Ω_2 $(\Omega_1+\Omega_2=\Omega)$ where carriers can be characterized by some different properties. It is easy to infer that because of this subdivision the instantaneous value of the drift velocity can be decomposed as

$$v_d(t)=v_1(t)p_1(t)+v_2(t)p_2(t), \tag{4}$$

where

$$v_i(t)=\int_{\Omega_i} v(\mathbf{p})F(\mathbf{p},t)d\mathbf{p}/\int_{\Omega_i} F(\mathbf{p},t)d\mathbf{p} \tag{5}$$

is the instantaneous average velocity of carriers inside the momentum volume Ω_i and

$$p_i(t)=\int_{\Omega_i} F(\mathbf{p},t)d\mathbf{p} \tag{6}$$

is the relative population of this volume. Due to the condition given by Eq. (2), the instantaneous values of the relative populations must satisfy the condition

$$p_1(t)+p_2(t)=1. \tag{7}$$

In the framework of such a two-group decomposition, the fluctuations of the drift velocity can be decomposed as

$$\delta v_d(t)=\delta v^{reg}(t)+\delta v^{part}(t), \tag{8}$$

where

$$\delta v^{reg}(t)=\delta v_1(t)\overline{p_1}+\delta v_2(t)\overline{p_2} \tag{9}$$

is the regular component describing fluctuations inside the groups, and

$$\delta v^{part}(t)=(\overline{v_1}-\overline{v_2})\,\delta p(t) \tag{10}$$

is the partition component describing fluctuations caused by intergroup transitions induced by scattering events when the average statistical velocities in the groups are different, $\overline{v_1}\neq\overline{v_2}$. Equation (10) takes into account that, due to the condition given by Eq. (7), fluctuations of the relative populations of the two groups are entirely correlated, $\delta p_1(t)=-\delta p_2(t)=\delta p(t)$.

Such a formal decomposition of carriers in momentum space is of physical meaning only in the case in which velocity fluctuations inside the groups, $\delta v_i(t)$, and fluctuations of the relative populations $\delta p(t)$ are statistically independent, that is, $\overline{\delta v_1(t)\,\delta v_2(t)}=0$ and $\overline{\delta v_i(t)\,\delta p(t)}=0$. Usually this takes place when the characteristic time of the intergroup exchange $\tau_g \gg \tau_i$ $(i=1,2)$, where τ_i is the characteristic relaxation time of velocity fluctuations inside the ith group. Under these conditions, the fluctuations of the relative occupation of regions in momentum space manifest themselves as an independent source of fluctuations with respect to the usual velocity fluctuations. Such a situation can be expected when the character of carrier motion in momentum space changes drastically between two kinds of dynamics that coexist simultaneously. Here, we will not enter into the details of the processes occurring inside groups, assuming only that the intergroup exchange time is longer than any other characteristic times in the system. In this case, the two-time correlation function describing the fluctuations of the relative populations of the two groups can be represented as

$$C_{\delta p\,\delta p}(t',t'')=\overline{p_1}\,\overline{p_2}e^{-|t'-t''|/\tau_g}. \tag{11}$$

Under stationary conditions, $\overline{p_i}$ and $\overline{v_i}$ are constant and the correlation function of drift velocity fluctuations takes the form

$$C_{\delta v\,\delta v}(t'-t'')=C^{reg}_{\delta v\,\delta v}(t'-t'')+(\overline{v_1}-\overline{v_2})^2\overline{p_1}\,\overline{p_2}e^{-|t'-t''|/\tau_g}, \tag{12}$$

where $C^{reg}_{\delta v\,\delta v}(t'-t'')=\overline{\delta v^{reg}(t')\,\delta v^{reg}(t'')}$. By applying the Wiener-Kintchine theorem to Eq. (12), one obtains the spectral density of velocity fluctuations[2–5] to be

$$S_{\delta v\,\delta v}(\omega)=S^{reg}_{\delta v\,\delta v}(\omega)+S^{part}_{\delta v\,\delta v}(\omega), \tag{13}$$

where

$$S^{part}_{\delta v\,\delta v}(\omega)=\frac{4(\overline{v}_1-\overline{v}_2)^2\overline{p}_1\overline{p}_2\tau_g}{1+\omega^2\tau_g^2} \tag{14}$$

is the contribution of the intergroup fluctuations to the total spectral density of drift velocity fluctuations. Thus, under stationary conditions the source of partition noise is proportional to a square of a group velocity difference and manifests itself as an additional low-frequency noise at $\omega<\tau_g^{-1}$. Since the intensity of the partition component of velocity fluctuations is proportional to the statistical averages of the group occupancies [see Eq. (14)], this noise component exhibits the maximum contribution when the occupancies are equal, i.e., $\overline{p}_1=\overline{p}_2=0.5$. Therefore, in the transition from one type of carrier dynamics in momentum space (one group) to the other one (second group), the appearance of an extra noise is expected, in full analogy with a phase transition. In semiconductors, where some scattering mechanism has a threshold character (optical-phonon emission, intervalley scattering, etc.) such a transition takes place with the increase of the electric-field strength when the carrier energy begins to exceed some threshold value. Usually such a transition manifests itself as a kink in the static velocity-field relation.[12]

Let us now generalize the partition noise described above to the case of the so-called *cyclostationary* conditions, when carriers are heated by a strong monochromatic MWEF of frequency *f*. Under these conditions, the statistical independence of velocity fluctuations inside the groups δv_i and of fluctuations in their population $\delta p(t)$ will take place only when $f\gg\tau_g^{-1}$. In the opposite case, a modulation of the average statistical value of the relative populations $\overline{p}_i(t)$ and, hence, of $\delta p(t)$ during a MWEF period will take place. Under the condition $f\gg\tau_g^{-1}$, only the average statistical value of the group velocities will keep the dependence on time during a MWEF period. Let us suppose, for simplicity, that the velocity response of each group to the MWEF is also harmonic with frequency *f*:

$$\overline{v}_i(t)=\overline{v}_i\cos(2\pi ft+\phi_i). \tag{15}$$

Without loss in generality, in the following we take $\phi_i=0$.

Now the two-time correlation function of velocity fluctuations takes the form

$$C_{\delta v\,\delta v}(t',t'')=C^{reg}_{\delta v\,\delta v}(t',t'')+(\overline{v}_1-\overline{v}_2)^2\overline{p}_1\overline{p}_2e^{-\frac{|t'-t''|}{\tau_g}}\times\cos(2\pi ft')\cos(2\pi ft''), \tag{16}$$

which, because of cyclostationary conditions, cannot be reduced to a single-time dependence given by the time difference $t'-t''$. In such a case it is convenient to use a correlation function that is symmetric with respect to the current phase $\phi=2\pi ft$ of the MWEF.[13] By replacing in Eq. (16) $t'=t-s/2$ and $t''=t+s/2$, where *t* and *s* are the phase and correlation times, respectively, and performing the Fourier transformation with respect to the correlation time *s*, one finally obtains the instantaneous spectral density, which depends on the phase time *t*:[13]

$$S_{\delta v\,\delta v}(t,\omega)=S^{reg}_{\delta v\,\delta v}(t,\omega)+\frac{1}{4}[S^{part}_{\delta v\,\delta v}(\omega-2\pi f)+S^{part}_{\delta v\,\delta v}(\omega+2\pi f)]+\frac{1}{2}S^{part}_{\delta v\,\delta v}(\omega)\cos(4\pi ft), \tag{17}$$

where $S^{part}_{\delta v\,\delta v}(\omega)$ is the partition noise contribution given by Eq. (14). As follows from Eq. (17), under cyclostationary conditions one-half of the low-frequency partition noise contribution is upconverted to the high-frequency region of the stationary component of the instantaneous spectral density of velocity fluctuations $\overline{S}_{\delta v\,\delta v}(\omega)$ (the term in square brackets, which is subdivided into two parts shifted symmetrically to positive and negative frequencies). The remaining half [last term in Eq. (17)] remains in the low-frequency region, but it corresponds to the nonstationary part of the spectrum, $S'_{\delta v\,\delta v}(t,\omega)=S_{\delta v\,\delta v}(t,\omega)-\overline{S}_{\delta v\,\delta v}(\omega)$, which in general is periodic with the MWEF frequency and contains a pronounced harmonic component at frequency $2f$. This behavior is taken as the signature of the upconversion phenomenon and can be used to identify the upconverted part of the spectrum, $S^{part}_{\delta v\,\delta v}(\omega)$, in the numerical simulation of fluctuation phenomena under cyclostationary conditions.

Indeed, under these conditions the instantaneous spectral density is always a periodic function of the phase time *t* and can be decomposed into a Fourier series as

$$S_{\delta v\,\delta v}(t,\omega)=\overline{S}_{\delta v\,\delta v}(\omega)+\sum_{n=1}^{\infty}S_n(\omega)\cos(2\pi fnt+\phi_n). \tag{18}$$

When the harmonics of the regular part $S^{reg}_{\delta v\,\delta v}(t,\omega)$ are negligible, the regular part and the upconverted spectrum [first and second terms in the right hand side of Eq. (18), respectively] constitute the stationary part [$\overline{S}_{\delta v\,\delta v}(\omega)$ term in Eq. (18)], while the partition noise spectrum [last term in Eq. (17)] will determine the frequency dependence of the second harmonic in Eq. (18), $S_2(\omega)=\frac{1}{2}S^{part}_{\delta v\,\delta v}(\omega)$.

The situation considered above corresponds to the case in which the average velocity of each group of carriers is of pure harmonic type, as indicated by Eq. (15). In a more general case it can contain also higher harmonics. Then, in Eq. (18) the stationary spectral density will contain upconversion peaks around harmonics kf ($k=3,5$, etc.) of the fundamental frequency *f*, while the time-dependent spectral density will contain contributions $S_n(\omega)$ at the doubled frequencies $n=2k$.

III. NUMERICAL RESULTS

Below we investigate two cases of relevant physical interest pertaining to bulk semiconductors subject to large-amplitude MWEF, where the upconversion of partition noise is clearly evidenced. As a first application, we consider bulk

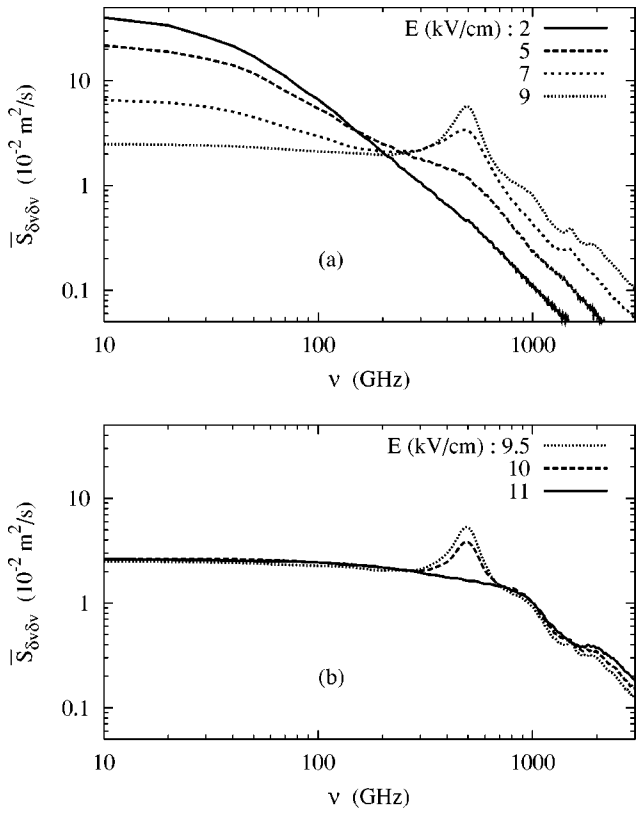

FIG. 1. (a) Appearance and (b) disappearance of the resonant-like peak of the stationary spectral density of velocity fluctuations calculated by the MC method when a MWEF with frequency $f = 500$ GHz and different amplitudes E is applied to bulk InN with a donor concentration $N_D = 10^{16}$ cm^{-3} at $T_0 = 80$ K.

n-InN at a lattice temperature $T_0 = 80$ K when the MWEF amplitude is sufficiently lower than that necessary for intervalley transfer to occur and most of the electrons are located at energies below that of the optical phonon. The parameters of the *n*-InN band structure and scattering mechanisms used in MC simulation are taken from Ref. 14.

Figure 1 presents the stationary component of the spectral density of velocity fluctuations, $\overline{S}_{\delta v\,\delta v}(\nu)$, calculated for increasing values of the amplitude E of a MWEF of frequency $f = 500$ GHz. For the lowest value $E = 2$ kV/cm [solid line in Fig. 1(a)] the carrier heating is insufficient for the electron energy ε to reach the optical-phonon energy $\hbar\omega_0 = 89$ meV. Accordingly, all the carriers remain in the energy region $\varepsilon < \hbar\omega_0$ (the so-called passive region), where because of the low lattice temperature the main sources of scattering are acoustic phonons and ionized impurities with an effective relaxation time of about 3 ps. As a consequence, the spectrum of velocity fluctuations is found to take the usual Lorentzian shape with the cutoff frequency given by the average scattering rate. With the increase of E, we found the onset of a peak at the MWEF frequency, $\nu = f$, and of minor peaks at higher harmonics [see Fig. 1(a)]. The peak reaches the maximum value at $E = 9$ kV/cm [dotted line in Fig. 1(a)] and then quickly disappears with a further increase of E [see Fig. 1(b)]. Finally, the spectrum takes again a near-Lorentzian shape [solid line in Fig. 1(b)]. Here the field amplitude is sufficiently high for all the carriers to acquire an energy $\varepsilon > \hbar\omega_0$ during every half period of the MWEF. Thus, carriers enter the so-called active region, where they quickly emit an optical phonon, and return back to the center of the passive region.

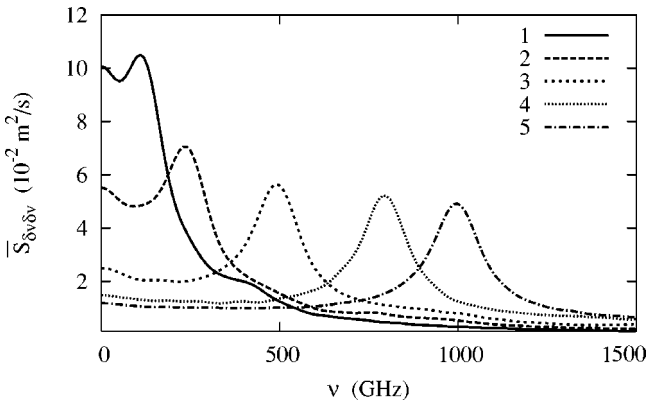

FIG. 2. Stationary spectral density of velocity fluctuations calculated for the same semiconductor of Fig. 1 under the application of MWEFs with frequencies $f = 133$, 250, 500, 800, and 1000 GHz and amplitudes $E = 2$, 4, 9, 15, and 19 kV/cm (curves 1–5), respectively.

As follows from Fig. 1, the peak at the MWEF frequency is practically superimposed to the Lorentzian part of the spectrum and can be considered as an extra noise attributed to an upconversion phenomenon. To support this interpretation, we have considered the dependence of the different spectral densities upon the frequency of the MWEF.

Accordingly, the stationary part of the fluctuation spectrum $\overline{S}_{\delta v\,\delta v}(\nu)$ and the upconverted noise spectrum, corresponding to $\frac{1}{2}S^{part}_{\delta v\,\delta v}(\nu)$ in Eq. (17), calculated for different frequencies f and amplitudes E of the MWEF, are presented in Figs. 2 and 3, respectively. Since in a harmonic field the change of carrier momentum during a free flight is proportional to $(E/f)\sin(2\pi ft)$, calculations are performed, keeping the ratio E/f nearly constant to provide similar trajectories of carrier free motion in the passive region at different frequencies f. Both $\overline{S}_{\delta v\,\delta v}(\nu)$ and $S'_{\delta v\,\delta v}(t,\nu)$ are directly obtained

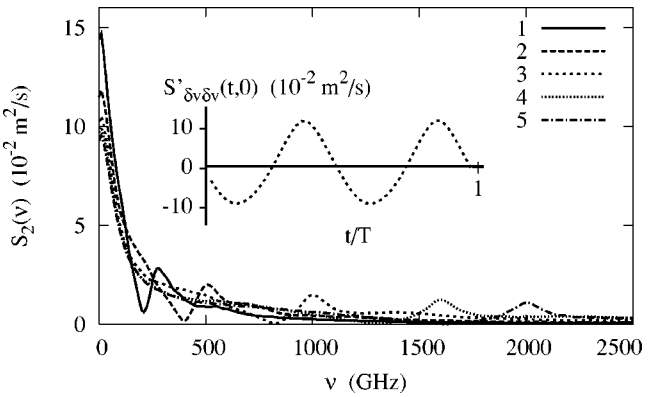

FIG. 3. Upconverted spectral density $\frac{1}{2}S^{part}_{\delta v\,\delta v}(\nu)$ calculated for the same conditions of Fig. 2 (curves 1–5). The inset shows the time dependence of $S'_{\delta v\,\delta v}(t,0)$ for case 3 during one period of the MWEF.

from the MC simulations, while $\frac{1}{2}S^{part}_{\delta v\,\delta v}(\nu)$ is calculated as the second harmonic $S_2(\nu)$ of the Fourier decomposition given by Eq. (18).

The peaks at the excitation frequency observed in the spectra of Fig. 2 are ascribed to the presence of an upconversion process. To validate this interpretation, the inset in Fig. 3 reports the time dependence of the instantaneous part of the fluctuation spectrum at zero frequency, $S'_{\delta v\,\delta v}(t,0)$, for a MWEF of 9 kV/cm and $f=500$ GHz. The inset clearly evidences that $S'_{\delta v\,\delta v}(t,0)$ exhibits a harmonic dependence upon t with frequency $2f$ and an amplitude that is twice higher than the value of $\overline{S}_{\delta v\,\delta v}(\nu)$ at $\nu=f$, in full agreement with the analytical model of upconversion previously described. These results confirm that the peak in Fig. 1 originates from an upconversion phenomenon. As follows from Fig. 2, the upconversion peak appears at $f\geqslant 100$ GHz as an additional superposition on the Lorentzian spectrum whose net contribution is represented by the first term in the right-hand side of Eq. (17). With a further increase of f, the relative contribution of the peak increases so that the maximum value of the upconverted noise exceeds several times the value of the regular contribution that originates from the velocity fluctuations inside different groups.

As demonstrated in Ref. 15, under the conditions for which we obtain the upconversion peak in $\overline{S}_{\delta v\,\delta v}(\nu)$, two groups of carriers with different behavior in response to the MWEF can be found in the passive region, i.e., at $\varepsilon(\mathbf{k})<\hbar\omega_0$. The first group consists of carriers that cannot reach the optical-phonon energy during half a period of the MWEF, so that their free motion always takes place inside the passive region of **k** space. The second group consists of carriers that synchronize their free motion with the field phase in such a way that each carrier emits at least one optical phonon during every half period, i.e., it reaches the active region boundary $\varepsilon=\hbar\omega_0$. The transfer of electrons between the two groups is a stochastic process driven by strongly randomizing scattering events occurring inside the passive region.

The formation and evolution of these two groups of carriers is illustrated in Fig. 4, which reports the distribution function along the field direction $f(k_x,t)$ during half a period of the MWEF at different time moments. Here, the peak of the distribution corresponds to the group of carriers that cannot reach the active region boundary, and the lower plateau corresponds to the group of carriers that emit an optical phonon twice per period.

The quite different dynamics of carriers inside the two groups is illustrated in Fig. 5, which shows the velocity time history of a single electron (solid line). For comparison, the dashed line plots the function $A\sin(2\pi ft)$ with a proper amplitude that evidences the velocity time dependence of the ballistic motion between scattering events. One can clearly detect two types of velocity sequences, which correspond to different groups. During the initial time period, from 0 to about 5 ps, the electron is in the group that emits an optical phonon each half of the MWEF period. During the final time period, from 5 to about 10 ps, the electron is in the other group which performs a nearly ballistic motion in momentum space. In accordance with the above model, the transitions between these two behaviors are responsible for the partition noise contribution [the second and third terms in Eq. (17)].

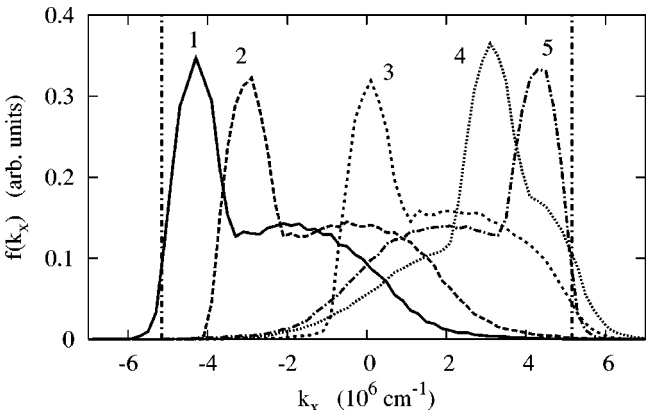

FIG. 4. Hot-electron distribution function in wave-vector space along the field direction, $f(k_x,t)$, calculated at different time moments corresponding to different phases (0, $\pi/4$, $\pi/2$, $3\pi/4$, π; curves 1–5, respectively) of the MWEF $E\sin(2\pi ft)$, with $E=9$ kV/cm and $f=500$ GHz. Vertical lines at $k=5.16\times10^6$ cm^{-1} refer to the boundaries of the passive region.

Therefore, the low-frequency part of the upconverted spectrum presented in Fig. 3, which shows a near-Lorentzian shape, is caused by the stochastic transitions of carriers between the two groups. In the same figure, the presence of the peaks at the double frequency $2f$ in $S_2(\nu)$ is attributed to the strong nonlinearity present in the system due to the coherent-in-time emission of two optical phonons at every MWEF period.

The second application concerns with the upconversion of partition noise related to the stochastic transitions between the lowest (Γ) and upper (X, L) valleys that occur in compound semiconductors when the amplitude of the MWEF is high enough for intervalley transitions to take place. To this purpose, Fig. 6 shows the stationary spectral density of velocity fluctuations calculated by MC simulations in bulk GaAs at $T_0=300$ K for a MWEF of $f=600$ GHz and in-

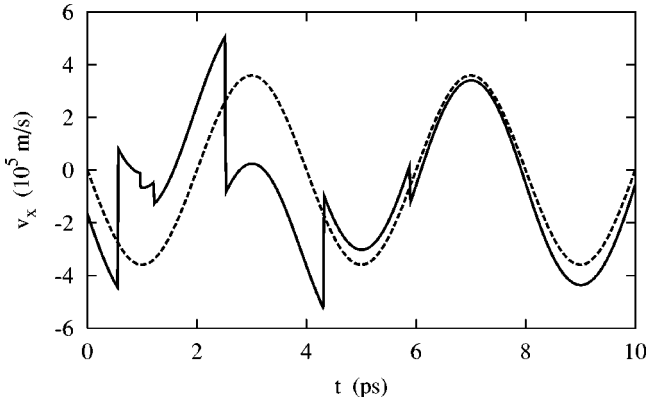

FIG. 5. Piece of time history of the parallel velocity (solid line) and function $A\sin(2\pi ft)$ with a proper amplitude (dashed line). $f=250$ GHz; $E=4$ kV/cm.

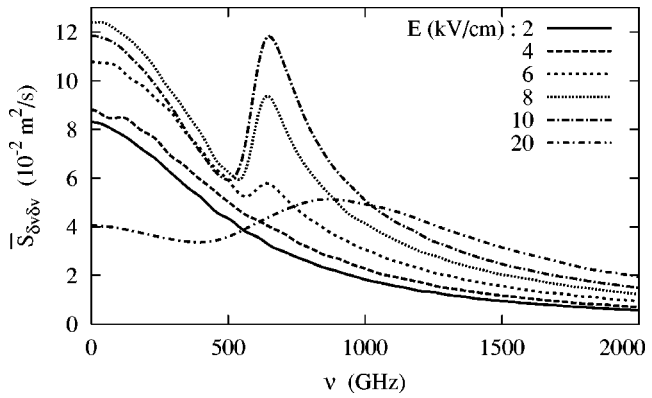

FIG. 6. Stationary spectral density of velocity fluctuations calculated when a MWEF with frequency $f=600$ GHz and different amplitudes E is applied to bulk GaAs with donor concentration $N_D=10^{16}$ cm^{-3} and $T_0=300$ K.

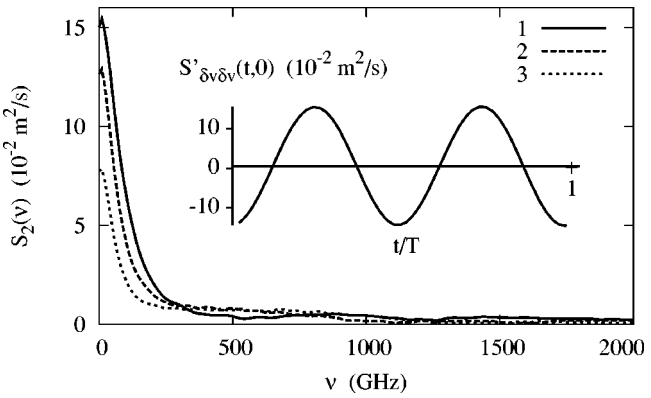

FIG. 8. Upconverted spectral density $S_2(\nu)=\frac{1}{2}S^{part}_{\delta v\,\delta v}(\nu)$ calculated for the same conditions of Fig. 7 for $f=600$, 800, and 1000 GHz (curves 1–3), respectively. The inset shows the time dependence of $S'_{\delta v\,\delta v}(t,0)$ in case 1 during one period of the MWEF.

creasing amplitude values. MC simulations take into account three spherically symmetric nonparabolic Γ, L, and X valleys. The parameters of the band-structure and scattering mechanisms of GaAs are taken from Ref. 16.

As follows from Fig. 6, at low amplitudes of the MWEF the spectrum shows the usual Lorentzian shape. When the field amplitude becomes sufficiently high for the onset of intervalley transfer, a peak at the MWEF frequency appears, initially the more pronounced the higher the field amplitude. Then, with the further increase of E above 10 kV/cm the peak starts to decrease and slightly shifts to higher frequencies (see the curve for 20 kV/cm). Such behavior is quite similar to that exhibited by the two groups under low-temperature optical-phonon scattering considered above (see Fig. 1). Again, the observed peak is attributed to an upconversion process. In this case the two groups of carriers exhibiting a very different velocity response to the MWEF correspond to those populating the lowest (Γ) and upper (L, X) valleys; therefore, the upconverted spectrum is associated with the random transitions between these groups.

To validate this interpretation, Figs. 7 and 8 provide additional information about the frequency and time dependence of the various components of the noise spectrum. The behavior of the stationary noise spectrum $\bar{S}_{\delta v\,\delta v}(\nu)$ when the MWEF frequency increases and the amplitude remains constant is illustrated in Fig. 7. For comparison, the static case is reported as a solid line. To keep a similar heating of carriers, the steady-state calculations were performed at the static electric field $E_0=7$ kV/cm$\approx E/\sqrt{2}$. Note that in the static case, the correlation function of velocity fluctuations exhibits a significant negative tail caused by (i) carrier transfer between the lower and upper valleys, where carriers have on average opposite deviations from the mean velocity, and (ii) carriers that return to the Γ valley with wave vector $k_x<0$, cross the Γ valley practically ballistically, and then are scattered back to upper valleys at $k_x>0$.[12,17–19] As a consequence, the spectral density of velocity fluctuations, $S_{\delta v\,\delta v}(\nu)$, exhibits a significant reduction of the low-frequency noise, a hot-carrier peak at $\nu\approx 300$ GHz, and a monotonous decrease in the highest-frequency region. With the increase of f this hot-carrier peak first shifts to a higher-frequency region (Fig. 7, dashed lines) and finally evolves (at $f\approx 500$ GHz) into a resonantlike peak around f where the correlation function of velocity fluctuations shows oscillations with frequency f. This proves the resonant origin of the peak. At a fixed value of E for $f\geqslant 500$ GHz the peak shifts linearly with f and becomes less pronounced (dash-dotted lines) since the ratio E/f starts to deviate considerably from the optimal value. Under optimal conditions, i.e., keeping the ratio E/f nearly constant at a value of about 15 kV cm^{-1} THz^{-1}, the peak is found to shift to a higher frequency, keeping practically the same amplitude in full analogy with the case of InN considered above. The peak originates from the upconversion process, as confirmed by the results reported in the inset of Fig. 8. Here, the zero-frequency value of the nonstationary part of the instantaneous spectral density $S'_{\delta v\,\delta v}(t,0)$ is found to exhibit purely harmonic behavior at a frequency $2f$, when this is higher than 500 GHz. For $f<500$ GHz the harmonic behavior of $S'_{\delta v\,\delta v}(t,0)$ is found to vanish, and thus no clear upconversion peak is observed in $\bar{S}_{\delta v\,\delta v}(\nu)$.

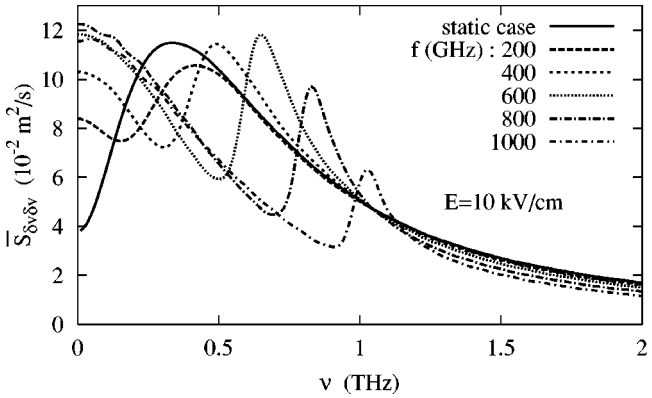

FIG. 7. Stationary spectral density of velocity fluctuations calculated for the same semiconductor of Fig. 6 and a MWEF with amplitude $E=10$ kV/cm and different frequencies $f=200$, 400, 600, 800, and 1000 GHz (curves 1–5), respectively.

As shown in Fig. 8, where the upconverted spectrum

$S_2(\nu)=\frac{1}{2}S^{part}_{\delta v\,\delta v}(\nu)$ is plotted for several frequencies of the electric field, in the case of intervalley transfer $S_2(\nu)$ takes a shape similar to that observed in Fig. 3 for the previous example. However, in Fig. 8 all higher harmonics $S_n(\nu)$ with $n\neq 2$ are negligible when compared with $S_2(\nu)$. As follows from Figs. 6–8, the maximum contribution of partition noise upconverted to the high-frequency range has practically the same magnitude of the regular noise.

The spectra presented in Fig. 8 are well described by the usual formula for partition noise $S(\omega)=S(0)/(1+\omega^2\tau_g^2)$ [see Eq. (14)] with $S(0)=0.15$, 0.13, and 0.8 m^2/s and $\tau_g=1.75$, 2.1, and 2.3 ps for curves 1–3, respectively. This further confirms that the spikes in Figs. 7 and 8 at $f\geqslant 500$ GHz are due to partition noise upconversion. Since the characteristic time τ_g of intergroup exchange is about 2 ps, the lower-frequency limit simply implies that to observe the upconversion the applied signal frequency must be higher than the characteristic rate of intergroup exchange, that is, $f\geqslant 1/\tau_g$.

It should be emphasized that in the case considered here, the population of *X* valleys is very low (less than 1%) so that main intervalley exchange is between Γ and *L* valleys. By considering the case of $E=10$ kV/cm and $f=600$ GHz, we compare the value of the characteristic intergroup time $\tau_g\approx 2$ ps with the lifetimes in Γ and *L* valleys $\tau_\Gamma=1.27$ ps and $\tau_L=0.44$ ps, respectively, as well as with the characteristic intervalley time $\tau_{inter}=0.33$ ps. From this comparison we conclude that the obtained intergroup time is significantly longer than the characteristic times of intervalley transfer. Therefore, in this case the intergroup exchange cannot be reduced to the simple intervalley exchange. Moreover, the systematic transformation of the hot-carrier peak into a resonant peak with the increase of the MWEF frequency (see Fig. 7) leads us to conclude that the same individual groups play an essential role in the formation of both kind of peaks. Thus, in full analogy with the first example considered previously, one can suppose that the two groups are formed by (i) low-energy Γ-valley electrons with insufficient energy for intervalley transfer to take place, which move in nearly a straight line while crossing the Γ valley due to the forward character of polar optical-phonon scattering and (ii) all other high-energy electrons that suffer very quick randomizing scatterings due to intense intervalley and intravalley (in upper valleys) scattering.

To support this microscopic interpretation, Fig. 9 shows the electron distribution, $n(\varepsilon)$, normalized to unity in energy space: $\int n(\varepsilon)d\varepsilon=1$, at three values of the MWEF phase. Two peaks in the energy distribution, corresponding to the two above-mentioned groups, are evident. The peak at low energy and its tail originate from low-energy Γ electrons, the energy of which is insufficient for intervalley transfer. The significant change of this peak with the MWEF phase is a consequence of the quasiballistic character of the carrier motion in this group. The peak at high energy is related to *L*-valley electrons and to high-energy Γ electrons involved into intervalley transfer. The change with phase of this peak is negligibly small and caused mostly by a small time modulation of the average populations of the two groups. This confirms that carrier exchange between these groups satisfies the stochastic character required to justify the analytical model.

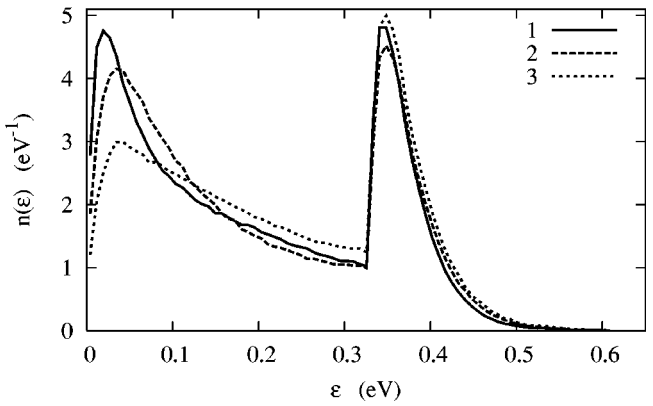

FIG. 9. Electron distribution in energy space at different phases ($\pi/4$, $\pi/2$, $3\pi/4$, curves 1–3, respectively) of the MWEF. $f=600$ GHz; $E=10$ kV/cm.

To illustrate the existence of the different time scales of carrier exchange, Fig. 10 shows the time dependence of the correlation function of fluctuations of the relative population of the Γ valley, $C_{nn}(s)$, calculated by the MC method for $E=10$ kV/cm and $f=600$ GHz (solid line). In full agreement with the analytical model of Sec. II [see Eq. (11)], $C_{nn}(0)=n_\Gamma n_L$, where $n_\Gamma=0.74$ and $n_L=0.26$ are the average relative populations of Γ and *L* valleys, respectively. As follows from Fig. 10, the initial decay of the correlation function is described by the short intervalley transfer time $\tau_{inter}=0.327$ ps (corresponding to the inverse of the slope of the figure). It originates from high-energy electrons undergoing fast intervalley transitions. Then, the final decay is described by a long characteristic time $\tau=1.75$ ps (corresponding to the inverse of the slope of the dashed line in the figure) associated with low-energy Γ electrons. It is just this time which is associated with the Lorentzian approximation of the upconverted spectrum presented in Fig. 8 (see curve 1), and,

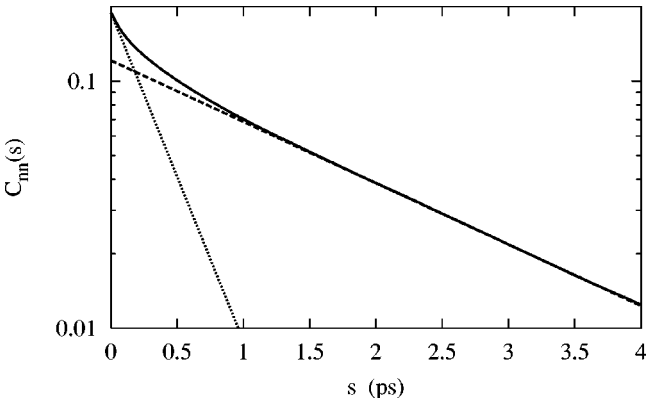

FIG. 10. Correlation function of fluctuations of the relative population of the Γ valley as a function of correlation time *s* (solid line). Dotted and dashed lines show the short- and long-time slopes of $C_{nn}(s)$. Calculations refer to a MC simulation performed at $f=600$ GHz, with $E=10$ kV/cm.

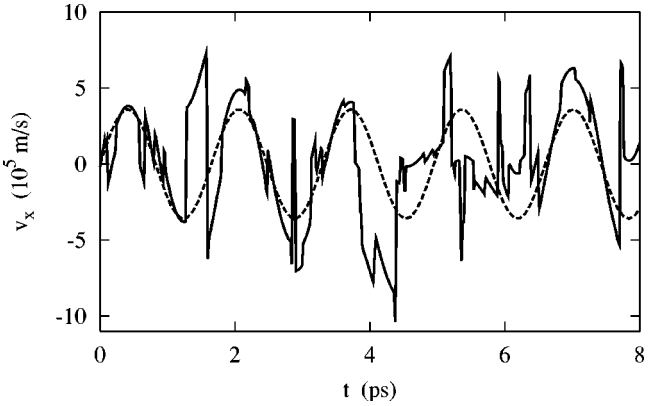

FIG. 11. Piece of time history of the parallel velocity (solid line) and function $A\sin(2\pi ft)$ with a proper amplitude (dashed line). $f=600$ GHz; $E=10$ kV/cm.

hence, it describes the electron exchange between the low- and high-energy groups.

The electron transitions between the two groups result in significant changes of the character of carrier motion in momentum space which, in accordance with the model presented above, sets the basis of the upconversion phenomenon. This is illustrated by Fig. 11, which shows the velocity time history of a single electron (solid line). For comparison, the dashed line plots the function $A\sin(2\pi ft)$ with a proper amplitude which evidences the amplitude modulation of the time history.

The upconversion phenomenon considered above determines the behavior of the spectral density of velocity fluctuations in the homogeneous case. Under conditions in which the spatial correlation of velocity fluctuations becomes negligible (see, for example, Ref. 20), the spectral density of velocity fluctuations is usually considered as the local (in real space) source of carrier diffusion noise. In turn, through the transfer fields this noise source determines the fluctuations of either the voltage drop at the open terminals or the current flow in the outside short circuit (the so-called Norton and Thenevin generators, respectively). These voltages (or current) fluctuations are the quantities usually measured in experiments. In the simple case of a homogeneous semiconductor resistor, the spectral density of current fluctuations, $S_{\delta I\,\delta I}(\omega)$, is given by

$$S_{\delta I\,\delta I}(\omega)=e^2\frac{A}{L}nS_{\delta v\,\delta v}(\omega), \tag{19}$$

where e is the electron charge, A and L are the cross-sectional area and the length of the resistor, n is the carrier concentration, and $S_{\delta v\,\delta v}(\omega)$ is the spectral density of velocity fluctuations. As follows from Eq. (19), the spectrum of $S_{\delta I\,\delta I}(\omega)$ is determined entirely by the spectrum of $S_{\delta v\,\delta v}(\omega)$. In more complicated cases of inhomogeneous semiconductor structures, the spectrum of current fluctuations is additionally modified by the transfer fields,[3,20] but, in any case, it is strongly influenced by the peculiarities of the $S_{\delta v\,\delta v}(x,\omega)$ spectra at the different positions x inside the structures.

This property of the spectrum of current fluctuations is illustrated in Fig. 12, which presents the spectra of two homogeneous n-GaAs resistors ($n=10^{16}$ cm^{-3}) with Ohmic contacts (curves 1 and 2 for $L=6$ and 1.2 μm and $A=10^{-13}$ and 2×10^{-14} m^2, respectively) and a submicron $0.3-0.6-0.3$ μm n^+nn^+ GaAs structure (curve 3, $n=10^{16}$ cm^{-3}, $n^+=2\times10^{17}$ cm^{-3}, and $A=10^{-14}$ m^2) calculated directly by an ensemble MC simulator, self-consistently coupled with a solution of the Poisson equation as described in Refs. 21–25. In the present case calculations were performed for an applied periodic voltage $U(t)=U_a\cos(\omega t)$ of frequency $f=600$ GHz. The amplitudes $U_a=6$, 1.2, and 0.6 V (curves 1–3) were chosen to obtain the same conditions of carrier heating as in bulk GaAs at $E=10$ kV/cm. For the sake of comparison, curve 4 shows the result calculated in accordance with Eq. (19) with $A/L=(1/6)\times10^{-7}$ m (value valid for the three cases reported in the figure) by using $S_{\delta v\,\delta v}(\omega)$ as obtained for bulk material at similar conditions (curve for $E=10$ kV/cm in Fig. 6).

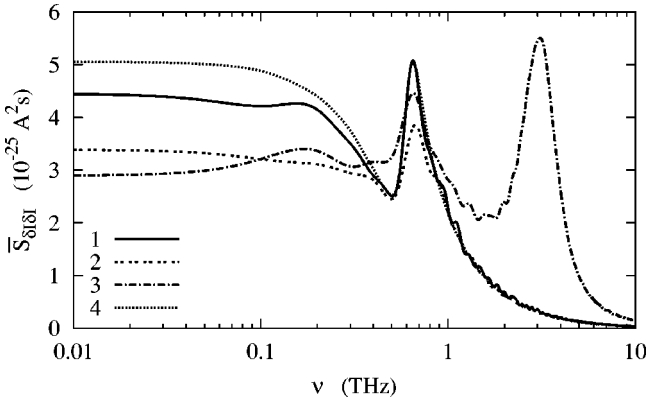

FIG. 12. Spectral density of current fluctuations for two terminal structures subjected to an applied voltage $U_a\cos(2\pi ft)$ with $U_a=6$, 1.2, and 0.6 V (curves 1–3) and $f=600$ GHz. Calculations are performed with a Monte Carlo simulator, self-consistently coupled with a Poisson solver. Curves 1 and 2 refer, respectively, to homogeneous n-GaAs resistors ($n=10^{16}$ cm^{-3}) with $L=6$ and 1.2 μm, and $A=10^{-13}$ and 2×10^{-14} m^2. Curve 3 refers to a submicron $0.3-0.6-0.3$-μm n^+nn^+ GaAs structure with $A=10^{-14}$ m^2, $n=10^{16}$ cm^{-3}, and $n^+=2\times10^{17}$ cm^{-3}. Curve 4 refers to $S_{\delta I\,\delta I}(\omega)$ for the same resistor as in curve 1, calculated in accordance with Eq. (19) by using $S_{\delta v\,\delta v}(\omega)$ obtained for bulk GaAs at $E=10$ kV/cm.

In all the cases shown in Fig. 12 the current spectrum $S_{\delta I\,\delta I}(\omega)$ contains the upconversion component, which appears around the frequency of the applied voltage $f=600$ GHz. For homogeneous resistors with $L\geqslant6$ μm the frequency dependence of the spectral density of current fluctuations is found to agree satisfactorily (within 10% at worst in the low-frequency region) with the result given by Eq. (19) and presented by curve 4. With the decrease of the resistor length, a systematic reduction of the power of fluctuations takes place (see curve 2 for $L=1.2$ μm). This reduction is due to the fact that, by decreasing L, the transit time τ_t necessary for a carrier to cross the resistor becomes comparable to the scattering time, thus suppressing the correlation of fluctuations at times longer than τ_t, i.e., a transition from diffusive to ballistic transport regime takes place.[26,27] In the n^+nn^+ structure, along with a similar low-frequency noise

reduction, an additional plasma peak at the highest frequencies (about 3 THz) appears, originated from carrier fluctuations around the n^+n homojunctions.[22] Thus, despite the various modifications of the current noise spectra, the upconversion phenomenon is confirmed in all cases as an output measurable quantity in real structures.

IV. CONCLUSIONS

We have reported a theoretical investigation of the upconversion of hot-carrier partition noise in bulk semiconductors operating under periodic large-signal conditions. It is shown that the low-frequency partition noise can result from fluctuations of the relative populations of momentum space regions (groups of carriers) characterized by essentially different dynamics of the single carrier motion (e.g., ballistic- or diffusive-like). Such a subdivision into different regions (groups), takes place under the dynamical heating of carriers by the microwave electric field when with the increase of an average energy of carriers an intense scattering mechanism, such as optical-phonon emission at low temperatures or electron transitions to upper valleys, becomes abruptly active above about a given amplitude of the electric-field strength. Under cyclostationary conditions, the subdivision into groups is proven to be invariant for a given value of the ratio between the amplitude and the frequency of the MWEF E/f. We show analytically, and validate by Monte Carlo simulations, that a purely harmonic behavior of the second harmonic of the instantaneous spectral density of velocity fluctuations at the double fundamental frequency should be considered a signature of the noise upconversion. In accordance with the picosecond time scale characteristic of hot-carrier partition noise, the upconversion takes place mostly around the THz frequency range.

We emphasize that since partition noise is intrinsic to the considered system, the upconversion process described in this work is an unavoidable phenomenon at the values of the MWEF frequency and amplitude analyzed here, and thus constitutes an intrinsic limitation for device applications. More precisely, as evidenced by MC calculations, the contribution of the upconverted partition noise at high frequencies is of the order of or even several times greater than the regular noise level. The range of frequencies and physical parameters considered in this work are accessible for an experimental test of the predicted phenomena.

Finally, we emphasize that the spectral density of velocity fluctuations in bulk materials calculated here constitutes, in turn, the noise source that enters into the impedance field method,[3,9,20] used to evaluate electronic noise in semiconductor devices. Thus, under the conditions for which the noise source exhibits the resonantlike peak, a similar behavior could be expected in inhomogeneous devices,[28] as confirmed here by MC simulations in an n^+nn^+ structure.

ACKNOWLEDGMENTS

The authors wish to acknowledge the financial support of the NATO collaborative-linkage Grant No. PST-.CLG.977520, the Spanish Secretaría de Estado de Educación y Universidades through Grant No. SAB2000-0164, the Dirección General de Investigación (MCyT) and FEDER through Project No. TIC2001-1754, the Consejería de Educación y Cultura de la Junta de Castilla y León through Project No. SA057/02, the Italy-Spain Joint Action of the MIUR Italy (Grant No. IT109) and MCyT Spain (Grant No. HI00-138), and the France-Lithuanian bilateral cooperation Grant No. 12864 of the French CNRS.

[1] A. van der Ziel, *Noise in Solid State Devices and Circuits* (Wiley, New York, 1986).
[2] P. J. Price, J. Appl. Phys. **31**, 949 (1960).
[3] W. Shockley, J. A. Copeland, and R. P. James, in *Quantum Theory of Atoms, Molecules and the Solid State*, edited by P. O. Lowdin (Academic, New York, 1966), p. 537.
[4] M. S. Gupta, J. Appl. Phys. **49**, 2837 (1978).
[5] J. P. Nougier, IEEE Trans. Electron Devices **41**, 2034 (1994).
[6] A. Hajimiri and T. H. Lee, IEEE J. Solid-State Circuits **33**, 179 (1998).
[7] S. Pérez, T. González, S. L. Delage, and J. Obregon, J. Appl. Phys. **88**, 800 (2000).
[8] S. Pérez, T. González, S. L. Delage, and J. Obregon, Semicond. Sci. Technol. **16**, L8 (2001).
[9] F. Bonani and G. Ghione, *Noise in Semiconductor Devices. Modeling and Simulation* (Springer, Berlin, 2001).
[10] P. Shiktorov, E. Starikov, V. Gružinskis, L. Reggiani, L. Varani, and J. C. Vaissière, Appl. Phys. Lett. **80**, 4759 (2002).
[11] S. Kogan, *Electron Noise and Fluctuations in Solids* (Cambridge University, Cambridge, England, 1996).
[12] W. Fawcett, A. D. Boardman, and S. Swain, J. Phys. Chem. Solids **31**, 1963 (1970).
[13] J. S. Bendat and A. G. Piersol, *Random Data* (Wiley, New York, 1986).
[14] B. E. Foutz, S. K. O'Leary, M. S. Shur, and L. F. Eastman, J. Appl. Phys. **85**, 7727 (1999).
[15] N. Ishida and T. Kurosawa, Jpn. J. Appl. Phys., Part 1 **64**, 2994 (1995).
[16] K. Brennan and K. Hess, Solid-State Electron. **27**, 347 (1984).
[17] G. Hill, P. N. Robson, and W. Fawcett, J. Appl. Phys. **50**, 356 (1979).
[18] R. Fauquemberdue, J. Zimmermann, A. Kaszynski, and E. Constant, J. Appl. Phys. **51**, 1065 (1980).
[19] R. Grondin, P. A. Blakey, J. R. East, and E. D. Rothman, IEEE Trans. Electron Devices **28**, 914 (1981).
[20] P. Shiktorov, E. Starikov, V. Gružinskis, T. González, J. Mateos, D. Pardo, L. Reggiani, L. Varani, and J. C. Vaissière, Riv. Nuovo Cimento **24** (9), 1 (2001).
[21] V. Mitin, V. Gruzhinskis, E. Starikov, and P. Shiktorov, J. Appl. Phys. **75**, 935 (1994).
[22] E. Starikov, P. Shiktorov, V. Gružinskis, J. P. Nougier, J. C. Vaissiere, L. Varani, and L. Reggiani, J. Appl. Phys. **79**, 242 (1996).
[23] T. González and D. Pardo, Solid-State Electron. **39**, 555 (1996).

[24] P. Shiktorov, V. Gružinskis, E. Starikov, L. Reggiani, and L. Varani, Phys. Rev. B **54**, 8821 (1996).
[25] V. Gružinskis, J. Liberis, A. Matulionis, P. Sakalas, E. Starikov, P. Shiktorov, B. Szentpali, V. Van Tuyen, and H. L. Hartnagel, Appl. Phys. Lett. **73**, 2488 (1998).
[26] B. R. Nag, S. R. Ahmed, and M. Deb Roy, Appl. Phys. A: Solids Surf. **A41**, 197 (1986).
[27] L. Varani, L. Reggiani, T. Kuhn, P. Houlet, T. González, and D. Pardo, Vuoto Sci. Tech. **XXII**, 116 (1992).
[28] S. Pérez and T. González, Semicond. Sci. Technol. **17**, 696 (2002).